How to cite: *Angew. Chem. Int. Ed.* **2023**, *62*, e202313037
doi.org/10.1002/anie.202313037

Peptides

Electrochemical Modification of Polypeptides at Selenocysteine

*Angus S. Mackay, Joshua W. C. Maxwell, Max J. Bedding, Sameer S. Kulkarni, Stephen A. Byrne, Lucas Kambanis, Mihai V. Popescu, Robert S. Paton, Lara R. Malins, Anneliese S. Ashhurst, Leo Corcilius, and Richard J. Payne**

Abstract: Mild strategies for the selective modification of peptides and proteins are in demand for applications in therapeutic peptide and protein discovery, and in the study of fundamental biomolecular processes. Herein, we describe the development of an electrochemical selenoetherification (e-SE) platform for the efficient site-selective functionalization of polypeptides. This methodology utilizes the unique reactivity of the 21st amino acid, selenocysteine, to effect formation of valuable bioconjugates through stable selenoether linkages under mild electrochemical conditions. The power of e-SE is highlighted through late-stage C-terminal modification of the FDA-approved cancer drug leuprolide and assembly of a library of anti-HER2 affibody conjugates bearing complex cargoes. Following assembly by e-SE, the utility of functionalized affibodies for in vitro imaging and targeting of HER2 positive breast and lung cancer cell lines is also demonstrated.

Introduction

Post-translational modifications (PTMs) of peptides and proteins provide a massive expansion in the structural and functional diversity of organismal proteomes.[1] As our understanding of the functional role of these PTMs has grown, there has been increased interest in the introduction of polypeptide modifications not incorporated by nature, such as fluorescent imaging tags and drug molecules, for the development of next-generation diagnostic and therapeutic agents. Critical to this pursuit is the availability of bioconjugation methods that enable chemo- and regioselective modification amongst the dense and diverse 'sea' of functionality present within the core set of 20 proteinogenic amino acids.[2] Such methods must be site-selective to prevent the generation of heterogeneous mixtures, proceed with high conversions to avoid challenging purification steps, and must also be competent under aqueous conditions that will not impair protein structure or function.

To date, chemoselective modification chemistry has been developed that enables functionalization of the N- and C-termini and almost all native amino acid side chains bearing polar or charged functionality within peptides and proteins.[2b–d,3] Lysine and cysteine side chains have been most frequently targeted, with their inherent nucleophilicity enabling facile conjugation to a wide variety of functionalities using *N*-hydroxysuccinimide esters and maleimides, respectively. The venerable Cu(I)-catalyzed azide-alkyne cycloaddition reaction,[4] strain-promoted azide-alkyne cycloaddition reaction,[5] and tetrazine chemistry[6] have also been used to link modifications to proteins, albeit on non-proteinogenic amino acid side chains. Despite the power of existing bioconjugation chemistries, truly site-specific modification of native proteinogenic amino acid side chains remains an enormous challenge, with most methods suffering from a lack of regioselectivity due to the high likelihood of a target amino acid residue appearing more than once in a protein sequence. For this reason, the native but very

[*] A. S. Mackay, J. W. C. Maxwell, M. J. Bedding, Dr. S. S. Kulkarni, Dr. S. A. Byrne, L. Kambanis, Dr. A. S. Ashhurst, Dr. L. Corcilius, Prof. R. J. Payne
School of Chemistry, The University of Sydney
Sydney, NSW 2006 (Australia)
E-mail: richard.payne@sydney.edu.au

A. S. Mackay, J. W. C. Maxwell, M. J. Bedding, Dr. S. S. Kulkarni, Dr. S. A. Byrne, L. Kambanis, Dr. L. Corcilius, Prof. R. J. Payne
Australian Research Council Centre of Excellence for Innovations in Peptide and Protein Science, The University of Sydney
Sydney, NSW 2006 (Australia)

Dr. M. V. Popescu, Prof. R. S. Paton
Department of Chemistry, Colorado State University
Fort Collins, CO 80523 (USA)

Assoc. Prof. L. R. Malins
Research School of Chemistry, Australian National University
Canberra, ACT 2601 (Australia)

Assoc. Prof. L. R. Malins
Australian Research Council Centre of Excellence for Innovations in Peptide and Protein Science, Australian National University
Canberra, ACT 2601 (Australia)

Dr. A. S. Ashhurst
School of Medical Sciences, Faculty of Medicine and Health, The University of Sydney
Sydney, NSW 2006 (Australia)

rarely incorporated amino acid selenocysteine (Sec), often dubbed the 21st amino acid, has emerged as an attractive option for performing chemo- and regioselective modification chemistry. Indeed, a range of arylation, cross metathesis, and alkylation bioconjugation approaches targeting Sec have been reported that primarily exploit its nucleophilicity and/or redox properties (Figure 1A).[7] However, many of these strategies require the use of transition metals or significant amounts of organic solvent (which can be incompatible with native polypeptides and proteins).

Synthetic electrochemistry has experienced a resurgence in recent years and is an attractive manifold for the site-selective late-stage functionalization of peptides.[8] The direct supply of electrons to a reaction removes the need for redox reagents, transition metal catalysts or photocatalysts, and enables precise tuning of redox parameters to the desired substrate. Electrochemical techniques also employ mild reaction conditions and display excellent functional group compatibility and scalability—highly attractive attributes when pursuing the modification of peptides and proteins. To date, reported methods in this rapidly evolving field have targeted proteinogenic functionality including tyrosine, tryptophan, and cysteine residues, as well as the C-terminus of peptides.[8e,9] While significant progress has been made, these approaches have mostly (with the notable exception of the powerful e-Y-click reaction)[9c,g,i] been applied on small peptide substrates, have often necessitated the use of organic solvent, and/or have offered limited regioselectivity. This highlights the ongoing need for new regioselective electrochemical strategies that are compatible with the full suite of proteinogenic functionality, including on larger polypeptide molecules, and that can be performed in aqueous solvent systems.

Herein, we report a mild electrochemical method for the chemoselective and regioselective modification of peptides and small proteins at selenocysteine (Figure 1B). The development of this proposed electrochemical modification chemistry took inspiration from a photocatalytic diselenide contraction (PDC) transformation recently developed in our laboratory (Figure 1A).[7a] The PDC method employs an iridium photocatalyst ($[Ir(dF(CF_3)ppy)_2(dtbpy)]PF_6$) together with a phosphine and irradiation at 450 nm to convert asymmetric or symmetric diselenide starting materials to their corresponding selenoether-linked products, with formal extrusion of a selenium atom. We sought to overcome key limitations of this methodology, including incompatibility with fluorogenic substrates and the use of expensive and poorly aqueous soluble photocatalysts, through the development of a low cost, atom economic, and biocompatible electrochemical method for site-selective functionalization of Sec residues, coined electrochemical selenoetherification (e-SE).

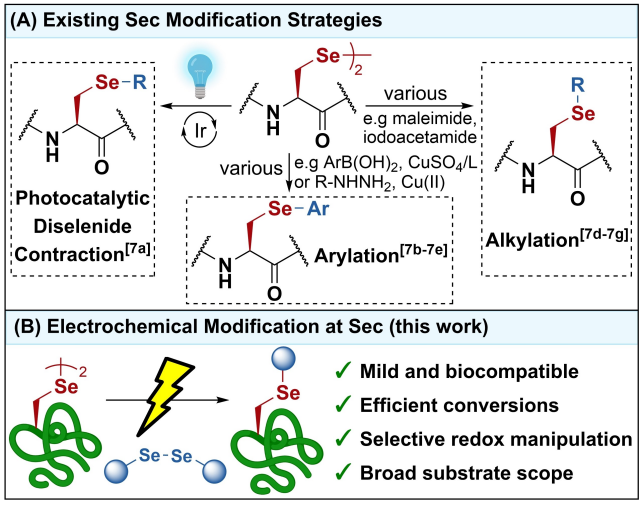

Figure 1. Strategies for the modification of Sec in peptides and proteins. A) Existing synthetic strategies for Sec modification. B) Electrochemical modification of polypeptides at Sec (this study).

Results and Discussion

We anticipated that the electrochemical protocol would proceed by an analogous reaction mechanism to PDC, beginning with the generation of a phosphorous-based radical cation. As such, we envisaged that it might be possible to initiate the e-SE conversion of peptide diselenides to stable, selenoether-linked polypeptides through anodic oxidation of a suitable phosphine.[10] We therefore began development of an e-SE approach that would operate in aqueous media by collecting a cyclic voltammogram (CV) of the highly water soluble derivative of triphenylphosphine, 3,3',3''-phosphanetriyltri(benzene-1-sulfonate) (TPPTS, **1**). A large anodic oxidation signal was observed at 1.05 V, corresponding to the oxidation of TPPTS to the radical cation (as seen in Figure 2A). We postulated that following oxidation, the electrochemical modification strategy would proceed through an analogous single-electron mechanism to that proposed for photocatalytic contraction reactions at Sec.[7a] Briefly, we hypothesized that the radical cation generated from anodic oxidation of the phosphine would induce homolytic diselenide cleavage, with cathodic reduction of the resultant selanyl radical generating one equivalent of a highly nucleophilic selenolate (Figure 2B). This reactive species could then attack the electrophilic selanyl phosphonium generated from diselenide cleavage to afford the desired selenoether-linked product and a phosphoryl selenide by-product.

Having determined the oxidation potential of TPPTS, we next sought to demonstrate the feasibility of the proposed e-SE transformation by attempting the dimerization of a model selenopeptide. To this end, a 22-residue peptide derived from the variable number tandem repeat (VNTR) of mucin-1 (a well-studied cancer antigen) bearing an N-terminal selenocysteine residue (MUC1 S1U, **2**) was chosen as a model to optimize the reaction conditions. Following a thorough voltage and phosphine screen (see the Supporting Information), we arrived at a set of general conditions for the desired e-SE transformation.

Specifically, when peptide **2** and TPPTS (8 equivalents) in a 0.5 M NaCl electrolyte solution were subjected to constant voltage electrolysis at 1.05 V using a commercially

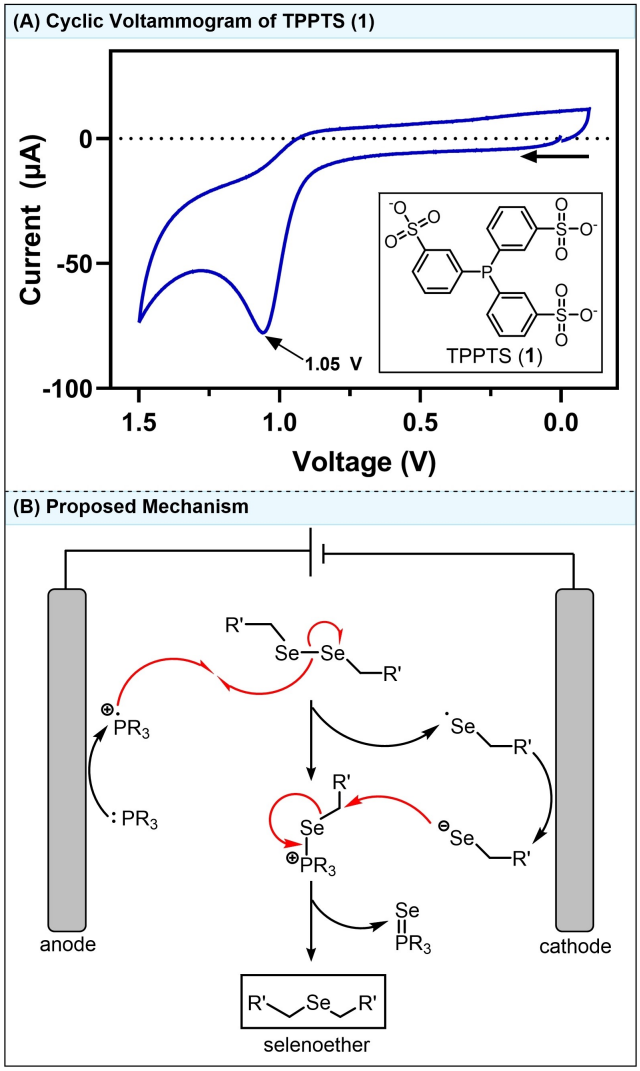

Figure 2. A) CV of TPPTS (**1**, inset) collected at 100 mV s^{-1} in 0.5 M $LiClO_4$. Arrow indicates scan direction. B) Proposed e-SE reaction mechanism.

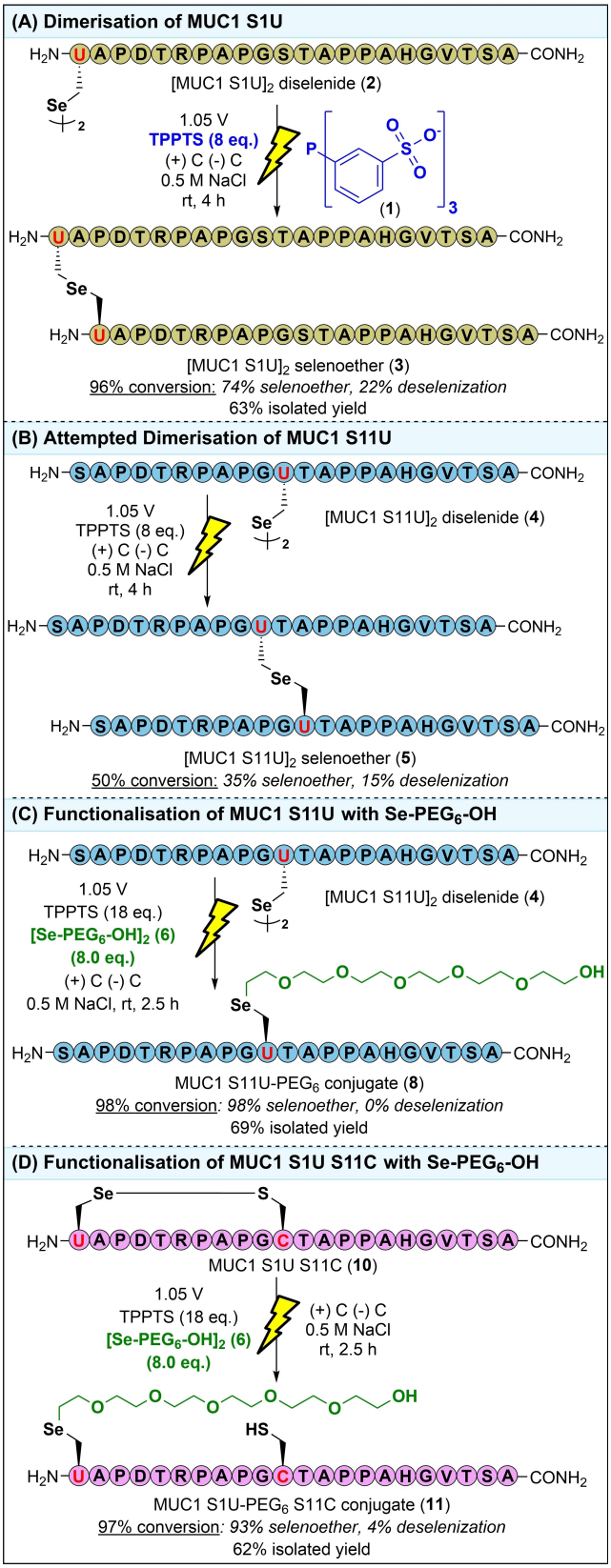

Scheme 1. Exploratory studies on the dimerization of A) MUC1 S1U (**2**) and B) MUC1 S11 U (**4**), and C) the functionalization of MUC1 S11U (**4**) and D) MUC1 S1U S11C (**10**) with $[Se\text{-}PEG_6]_2$ (**6**). Note: owing to the small scale of the reactions, UPLC-MS analysis was utilized as the primary means of tracking reaction progress (see the Supporting Information).

available IKA ElectraSyn 2.0 instrument equipped with graphite electrodes, 74 % conversion to the desired selenoether-linked dimeric product **3** was observed, together with 22 % deselenization, whereby the selenocysteine residue had been converted to alanine[11] (Scheme 1A). Of note, this transformation displayed impressive functional group tolerance, proceeding in the presence of a range of reactive functionalities including the imidazole side chain of histidine, guanidine motif in arginine, and unprotected amine and carboxylic acid moieties. Following purification by reversed-phase HPLC, selenoether dimer **3** was isolated in 63 % yield. Importantly, we also performed a series of control experiments that showed that the phosphine, electrolyte (NaCl), and electrolysis were all essential for selenoether generation (Table 1).

Having highlighted the potential of this electrochemical platform for effecting peptide dimerization, we next attempted to dimerize a model mucin-1 VNTR peptide

Table 1: Control experiments for the electrochemical dimerization of MUC1 S1U (**2**) at selenocysteine.

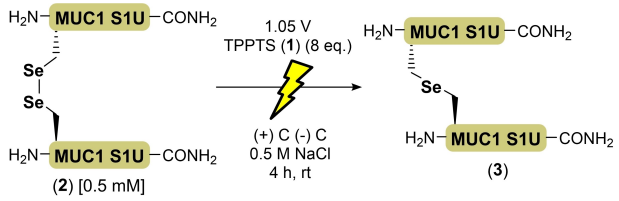

Deviation from standard conditions[a]	Conversion into MUC1 S1U selenoether **3**	Deselenization
none	74%	22%
no phosphine	not detected	not detected
no electrolysis	<5%	<5%
H_2O (no NaCl)	28%	<5%

[a] Standard conditions: constant voltage electrolysis, 8 equivalents TPPTS (**1**), 0.5 M NaCl electrolyte, graphite electrodes, 0.5 mM peptide concentration.

bearing an internally located selenocysteine residue (MUC1 S11U, **4**). However, under the previously optimized conditions, only 35% conversion to the desired selenoether product **5** was observed, alongside undesired deselenization (15%; Scheme 1B). This difference in conversion compared to MUC1 S1U was rationalized to be a result of the more sterically encumbered nature of the internally located selenocysteine. Although this limited the utility of the e-SE reaction for dimerizing larger systems, we reasoned that it could be a powerful method for the modification of polypeptides with a range of functionalities to afford asymmetric selenoether products.

In order to effect e-SE-based functionalization, it was envisaged that a polypeptide diselenide could first be mixed with a small molecule diselenide. We hypothesized that an excess of the small molecule diselenide could be used to favor formation of the asymmetric polypeptide-small-molecule diselenide through diselenide metathesis, and in turn promote selectivity for the 'cross-coupled' asymmetric polypeptide-small-molecule selenoether product over homodimerization of the polypeptide substrate or unwanted deselenization.[7a] It should be noted that some of the excess small molecule diselenide that does not exchange could also convert to the corresponding selenoether dimer during the course of the reaction. A key benefit of the selenoether linkages generated by e-SE is that they are not susceptible to redox exchange reactions with thiol and selenol nucleophiles, meaning that the attached cargo cannot be easily displaced. In contrast, diselenide-linked bioconjugates are redox active and can therefore undergo metathesis leading to loss of the desired payload. This is of particular concern given the high thiol concentrations (e.g. [glutathione] = 1–10 mM[12]) in cellular environments that would promote the dissociation of diselenide conjugates.

We first sought to demonstrate the feasibility of the functionalization workflow by subjecting a mixture of MUC1 S1U (**2**) and hexaethylene glycol diselenide [Se-PEG_6]$_2$ (**6**, 8 equivalents) to the optimized e-SE conditions developed for dimerization. Constant voltage electrolysis at 1.05 V provided near quantitative conversion to the desired asymmetric MUC1-PEG_6 selenoether (**7**) in 2 h with no detectable deselenization by-product (see the Supporting Information). Due to the potential for variability in reaction efficiencies between different ElectraSyn devices, we performed replicate experiments in two independent laboratories at the University of Sydney (Sydney) and the Australian National University (Canberra). Consistent conversions were observed across three different ElectraSyn systems, albeit with reaction times ranging from 2 to 8 h (see the Supporting Information). Pleasingly (and in contrast to our attempted dimerization), MUC1 S11U (**4**) was also compatible with this functionalization protocol, with 2.5 h of constant voltage electrolysis delivering 98% conversion to the corresponding MUC1-PEG_6 internal selenoether (Scheme 1C). Subsequent HPLC purification afforded site-specifically modified, selenoether-linked PEG_6 conjugate **8** in 69% isolated yield.

Given the similar reactivity profiles of cysteine and selenocysteine, we also sought to demonstrate the compatibility of the e-SE protocol with cysteine residues and to confirm that the reaction proceeds with complete chemoselectivity for Sec in the presence of Cys. First, a MUC1 mutant bearing an N-terminal cysteine residue (MUC1 S1C, **9**) was subjected to optimized e-SE functionalization conditions with [Se-PEG_6]$_2$ (**6**)—no modification of MUC1 peptide **9** was observed (see the Supporting Information). In contrast, e-SE modification of a mutant containing both Cys and Sec residues (MUC1 S1U S11C, **10**) proceeded with exclusive modification at the Sec residue to generate MUC1 S1U-PEG_6 selenoether S11C **11**, as confirmed by UPLC-MS analysis following HPLC purification and trypsin digestion (Scheme 1D, see the Supporting Information).

Having optimized conditions for efficient e-SE functionalization chemistry, we next performed a series of NMR spectroscopy experiments and quantum chemical calculations to further interrogate the mechanism of the electrochemical transformation proposed in Figure 2B. Analysis of a competent e-SE reaction mixture by ^{31}P NMR confirmed the presence of the expected TPPTS selenide by-product (see the Supporting Information). Furthermore, NMR analysis of a model peptide selenoether dimer formed from an e-SE reaction showed that the reaction proceeds with retention of stereochemistry at the α-carbon center of Sec. These data are consistent with e-SE proceeding by our proposed mechanism, rather than through an alternate pathway involving a dehydroalanine intermediate (see the Supporting Information). Density functional theory (DFT) calculations of a series of activation energy barriers also support our mechanistic hypothesis, implicating the selenolate species as a crucial and competent reaction intermediate and, in line with our experimental results, highlighting the influence of sterics at the reaction site on the outcome and selectivity profiles of e-SE dimerization and functionalization reactions (see the Supporting Information). Redox potentials of postulated electroactive species were also computed and found to align with experimental CV data

and the potential that was applied to promote the e-SE reactions (see the Supporting Information).

We next sought to highlight the utility of the e-SE technology for late-stage modification of a target of clinical interest. For this purpose, we selected leuprolide, a gonadotropin-releasing hormone analogue that is on the WHO List of Essential Medicines and widely used in the treatment of prostate and breast cancer.[13] Installation of a diselenide handle at the C-terminus afforded a close structural analogue of the leuprolide drug, with substitution of a single hydrogen atom for a selenium atom. This system was also selected to highlight that the methodology is not limited to functionalization of selenocysteine residues but can also be used for challenging C-terminal modification of polypeptides. Leuprolide diselenide **12** was subjected to the optimized electrochemical selenoetherification protocol, with a modified 1:1 v/v MeCN:H_2O solvent system used to ensure the solubility of both **12** and the small molecule diselenides (see the Supporting Information for further synthetic details). Pleasingly, the mild electrochemical conditions facilitated selective modification with high conversions for both a PEG_4 moiety (**13**, 83%) and biotin affinity label (**14**, 83%; Scheme 2). These experiments serve as an important proof of concept for C-terminal modification and act to validate the compatibility of this strategy with small, druglike peptides and small molecule diselenide substrates.

We next set out to assess the applicability of the e-SE platform for late-stage modification of larger targets. $Z_{HER2:342}$, a Z-domain affibody evolved to target the HER2 receptor,[14] bearing an additional N-terminal selenocysteine residue (Sec-zHER2, **15**) was chosen as a larger system to explore the scope of the chemistry. HER2-selective bioconjugates are of significant interest as diagnostic and therapeutic agents, owing to the association of abnormal expression and signaling of the HER2 receptor with the development, progression, enhanced invasiveness, and treatment resistance of several forms of cancer.[15] Functionalization of Sec-zHER2 (**15**) was performed under the optimized constant voltage e-SE conditions, with attachment of $[Se\text{-}PEG_6]_2$ (**6**) serving as an initial pilot example. Gratifyingly, the reaction proceeded with 90% conversion, affording the desired zHER2-PEG_6 selenoether-linked conjugate (**16**) in 77% isolated yield following HPLC purification (Figure 3). Following tryptic digestion, sequencing by tandem mass spectrometry was used to verify that the PEG_6 moiety was appended to the N-terminal Sec residue (see the Supporting Information). Additionally, the circular dichroism (CD) spectra of **16** and an unmodified alanine mutant (Ala-zHER2, **17**) were near identical, confirming that **16** retains its α-helical fold even after functionalization through e-SE (see the Supporting Information). We then applied our conditions to enable the efficient assembly of a 7-member library of modified affibodies (**16**, **18**–**23**), with excellent conversions and minimal unwanted deselenization (Figure 3). Notably, modification with a DOTA cage and subsequent chelation of yttrium was achieved in one-pot without intermediate purification to afford **20**, while successful labelling with a TAMRA probe (**21**) demonstrates the compatibility of e-SE with fluorogenic substrates. We also attached the structurally complex BRD-4-targeting PROTAC MZ1 and the highly selective integrin-targeting cyclic peptide (cyclic RGDyK), to afford the corresponding affibody-PROTAC (**22**) and peptide-protein (**23**) conjugates, respectively. These latter two examples highlight the utility of the e-SE method for the site-selective conjugation of large molecules. As for zHER2-PEG_6 conjugate **16**, products **18**–**23** retained their characteristic α-helical fold following functionalization (see the Supporting Information for CD spectra). Taken together, this library of site-selectively modified zHER2 constructs showcases the wide substrate scope of e-SE and the potential utility of the methodology for generating conjugates with applications in biology and medicine, e.g. as imaging agents and diagnostics.

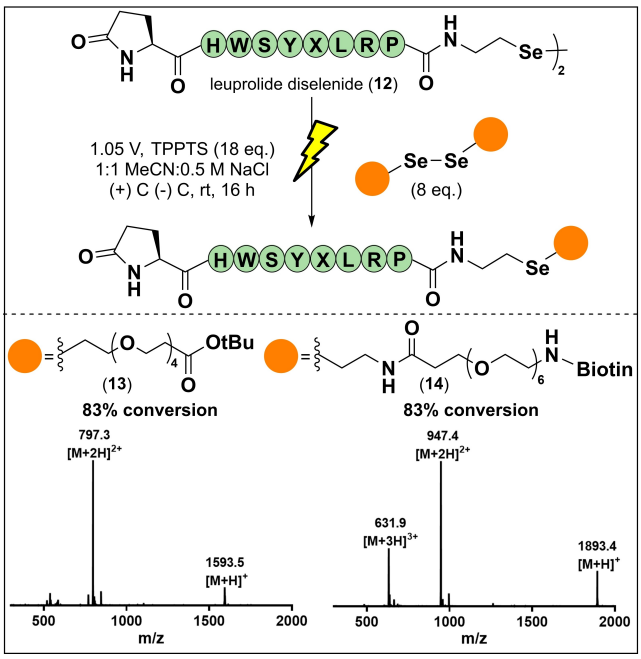

Scheme 2. Assembly of modified leuprolide conjugates **13** and **14**. ESI-MS(+) spectra of purified **13** and **14** following e-SE functionalization are shown as insets. Note: X = D-Leu.

The activity and application of a selection of the modified zHER2 conjugates was then assessed (Figure 4). First, we measured the affinity of **16** and **18**–**23** for the HER2 receptor using surface plasmon resonance (SPR). Pleasingly, the measured affinities of **16**, **18**, **19**, and **20** (K_D = 26–111 pM) were comparable to both unmodified Ala-zHER2 (**17**, K_D = 43 pM) and the dissociation constant reported when the $Z_{HER2:342}$ affibody was first evolved (K_D = 22 pM),[14] suggesting that attachment of small cargo does not significantly impair HER2 binding (Figure 4i). Unsurprisingly, a decrease in binding affinity was observed for conjugates **21**, **22**, and **23** bearing larger modifications—cargoes which may disrupt key interactions at the zHER2-HER2 binding interface (K_D = 273–2010 pM).

Given confirmation of affinity for the HER2 receptor by SPR, we next turned our attention to in vitro validation of the diagnostic and therapeutic value of the selenoether-linked zHER2 conjugates. To begin, we hypothesized that

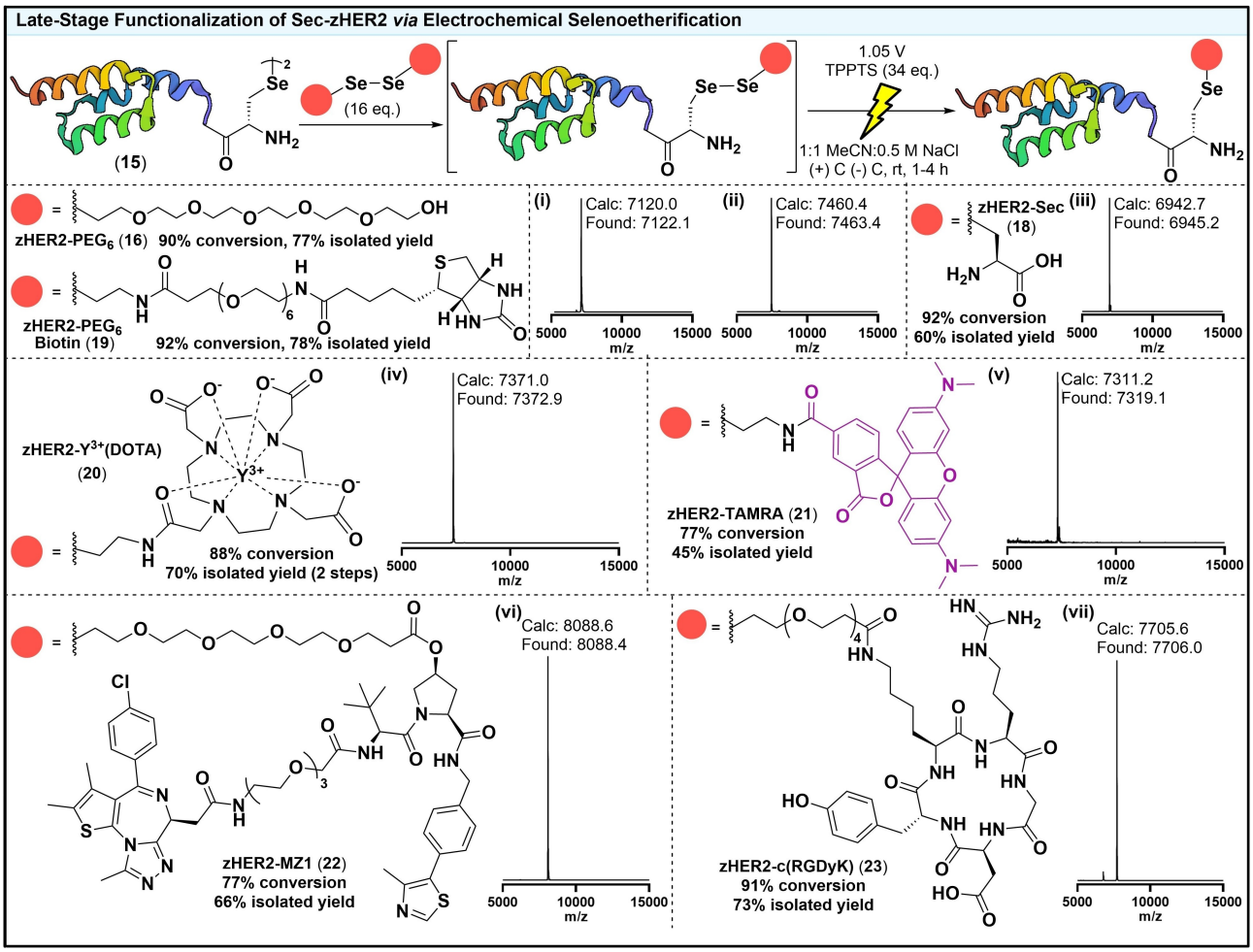

Figure 3. Electrochemical selenoetherification for the late-stage functionalization of the anti-HER2 affibody Sec-zHER2 (**15**). MALDI-TOF MS(+) spectra of purified conjugates following e-SE functionalization with i) PEG_6 (**16**), ii) PEG_6-Biotin (**19**), iii) selenocysteine (**18**), iv) Y^{3+} (DOTA) (**20**), v) TAMRA (**21**), vi) MZ1 (**22**), and vii) cyclic RGDyK (**23**) are shown as insets.

zHER2-TAMRA conjugate **21** would be a highly effective probe for the detection and relative quantification of HER2 expression across multiple breast cancer cell lines. Such tool compounds are of interest as overexpression of the HER2 oncogene is strongly protumorigenic and increasing levels of the receptor are correlated with poor prognosis.[15c] It should be noted that despite the decrease in binding affinity relative to unmodified zHER2 (see above), **21** retained sub-nanomolar affinity for HER2. The fluorescently labelled affibody **21** was first used to confirm the relative expression levels of HER2 on AU565$^{(HER2\text{-}High)}$, MDA-MB-453$^{(HER2\text{-}Med)}$, and MCF-7$^{(HER\text{-}Low)}$ breast cancer cells by flow cytometry.[16] Pleasingly, zHER2-TAMRA **21** was able to distinguish between the differing HER2 expression patterns on the cell lines, validating that the selenoether-linked TAMRA conjugate binds selectively to HER2 and can be used to detect and assess its relative abundance in vitro (Figure 4ii).

Following the successful use of **21** in flow cytometry detection of HER2, we sought to explore its utility as an immunofluorescent probe for cellular imaging of HER2. To this end, Calu-3 cells (a lung cancer cell line known to overexpress HER2) were treated with zHER2-TAMRA (**21**) and a nuclear stain and then visualized using live confocal microscopy. Only the cells that had been treated with **21** exhibited membrane-localized fluorescence in the TAMRA channel (561 nm; Figure 4iii). We next explored the ability of conjugate **20** bearing a DOTA cage with chelated yttrium to selectively distribute yttrium to HER2-overexpressing cell lines. Following incubation with **20**, the panel of breast cancer cells was analyzed using mass cytometry to measure cellular yttrium delivery (Figure 4iv). Considerably more yttrium was detected in the AU565$^{(HER2\text{-}High)}$ sample over the MDA-MB-453$^{(HER2\text{-}Med)}$ and MCF-7$^{(HER\text{-}Low)}$ samples, suggesting that zHER2-DOTA (**20**) is an effective agent for the selective delivery of yttrium (an element widely used in radiotherapy). Due to the versatile nature of DOTA as a chelating ligand, this class of constructs could be readily adapted for future applications in PET imaging and/or radionuclide delivery through complexation of different species.

As a final demonstration of the capabilities of this new methodology, we sought to construct an affibody-drug

Functional Activity of zHER2 Conjugates

(i) HER2 Binding Affinity

zHER2-conjugate	K_D (pM)	k_{on} (M^{-1} s^{-1}) x 10^6	k_{off} (s^{-1}) x 10^{-4}
Ala-zHER2 (**17**)	43 ± 17	4.9 ± 1.7	2.14 ± 0.34
PEG_6 (**16**)	52.6 ± 9.3	6.0 ± 1.4	3.2 ± 1.2
Sec (**18**)	25.8 ± 1.6	4.17 ± 0.70	1.08 ± 0.25
Biotin (**19**)	111 ± 17	2.01 ± 0.29	2.231 ± 0.062
Y^{3+}(DOTA)(**20**)	47.0 ± 0.16	4.4 ± 0.47	2.04 ± 0.14
TAMRA (**21**)	804 ± 27	1.369 ± 0.007	0.110 ± 0.032
MZ1 (**22**)	2010 ± 140	0.1181 ± 0.0030	2.37 ± 0.20
c(RGDyK) (**23**)	273 ± 66	0.96 ± 0.94	2.61 ± 0.30

(ii) Detection and Relative Quantification of HER2 Expression

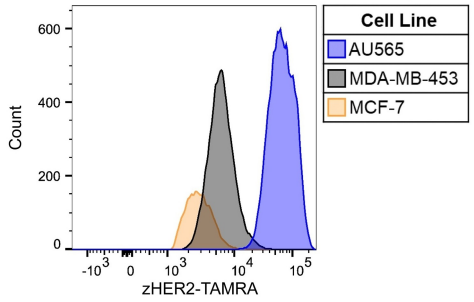

(iii) Cellular Imaging of HER2

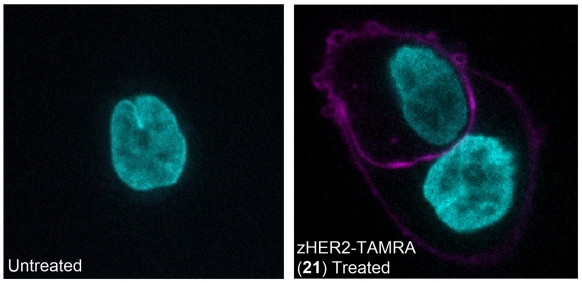

(iv) HER2-Selective Yttrium Delivery

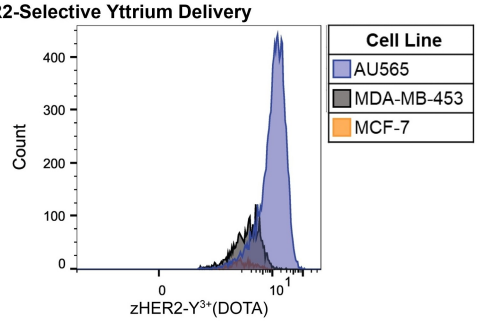

Figure 4. Evaluation of the functional activity of the selenoether-linked zHER2 conjugates. i) Affinity data for Ala-zHER2 **17** and zHER2 conjugates **16**, **18**–**23** against human IgG1 Fc-tagged HER/ERBB2 immobilized on a Series S Protein A Sensor SPR Chip. K_D, k_{on}, k_{off} values determined using a kinetic fit assuming 1 : 1 binding stoichiometry. ii) Comparison of HER2 surface expression by MCF-7, MDA-MB-453 and AU565 cell lines using zHER2-TAMRA (**21**) staining and detection by flow cytometry. iii) Fluorescence imaging of Calu-3 cancer cells using confocal microscopy. Cells were treated with zHER2-TAMRA (**21**; magenta) and/or NucBlue (Hoechst 33342; blue) prior to imaging. iv) Comparison of yttrium positive MCF-7, MDA-MB-453 and AU565 cells following incubation with Y^{3+}(DOTA) (**20**) and detection by mass cytometry.

conjugate. Antibody drug conjugates (ADCs) are enormously valuable bifunctional therapeutic agents that are capable of selectively delivering cytotoxic compounds to cancer cells.[17] Antibody-mimetic drug conjugates (e.g. affibody-drug conjugates) have also attracted significant attention as alternative modalities with the potential for improved control over the modification site and tissue penetration.[18] The anti-cancer agent monomethyl auristatin E (MMAE), which has been used clinically in ADCs, was selected for attachment to Sec-zHER2 using e-SE. We designed a construct containing this cytotoxic payload appended via a cathepsin B-cleavable self-immolative linker (Val-Cit-PAB), with incorporation of a diselenide-containing polyethylene glycol chain to enable subsequent e-SE conjugation (**24**, see the Supporting Information for detailed synthetic procedure). The challenging affibody-drug conjugation was then attempted using the optimized electrochemical modification protocol (Scheme 3). Pleasingly, e-SE functionalization proceeded with 89 % conversion after 1 h, delivering zHER2-PEG-Val-Cit-PAB-MMAE (hereafter zHER2-MMAE, **25**) in 82 % isolated yield following purification by reversed-phase HPLC. With the desired conjugate in hand, the antimitotic effect of zHER2-MMAE (**25**) was then examined against AU565$^{(HER2\text{-}High)}$, MDA-MB-453$^{(HER2\text{-}Med)}$, and MCF-7$^{(HER2\text{-}Low)}$ breast cancer cell lines. We first established that MMAE alone displayed similarly potent cytotoxicity across the three cell lines (see the Supporting Information), affirming the need for selective delivery of the MMAE cytotoxin. In contrast, the cytotoxicity of **25** correlated strongly with HER2 expression, with the selenoether-linked conjugate displaying dramatically improved efficacy against the AU565$^{(HER2\text{-}High)}$ cells over the other cell lines (Scheme 3iv). This powerful example highlights the utility of the e-SE manifold as a means of accessing polypeptide-drug conjugates for biomedical applications.

Conclusion

In summary, we have developed a robust electrochemical strategy for the chemoselective and regioselective modification of polypeptides. This late-stage functionalization methodology, termed electrochemical selenoetherification (e-SE), affords stable selenoether-linked conjugates through contraction of diselenide bonds with the formal loss of a selenium atom. The e-SE methodology employs mild reaction conditions and displays excellent selectivity and compatibility with a broad range of functionality, including all 20 common proteinogenic amino acids. We have demonstrated that e-SE can facilitate clean and efficient attachment of diverse cargoes (e.g. biotin, fluorophores, DOTA, cytotoxic drugs, PROTACs, peptides) across a number of complex substrates. Assembly of these valuable bioconjugates enabled the utility of anti-HER2 affibody-payload constructs to be studied in vitro and highlights the potential

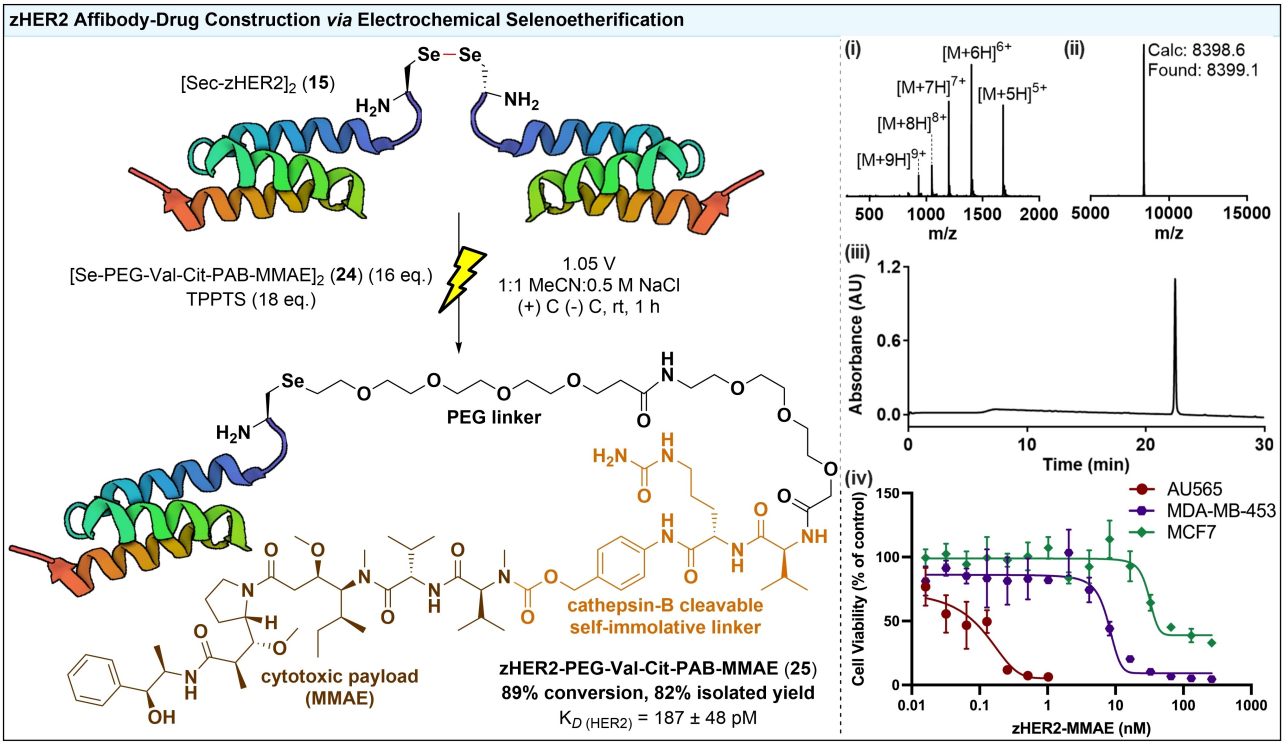

Scheme 3. zHER2 affibody-drug conjugate synthesis by e-SE. i) ESI-MS(+), ii) MALDI-TOF MS(+) and iii) analytical HPLC trace of zHER2-MMAE (**25**). iv) Cell viability of MCF-7, MDA-MB-453 and AU565 cells after incubation with various doses of zHER2-MMAE (**25**) for 96 h, determined by Alamar Blue HS. Cell viability for each cell line was normalized to untreated controls and plotted as the mean (±SD) of four technical replicates.

for broad applicability of this methodology in the study of bioactive polypeptide conjugates.

Supporting Information

The authors have cited additional references within the Supporting Information.[19]

Acknowledgements

This work was supported by the Australian Research Council Centre of Excellence for Innovations in Peptide and Protein Science (ARC Grant No. CE200100012 to L.R.M. and R.J.P.), by the Australian Government Research Training Program (RTP; scholarships to A.S.M., J.W.C.M., M.J.B., and L.K.) and by the John A Lamberton Research Scholarship (A.S.M., J.W.C.M., M.J.B., and L.K.). R.S.P. acknowledges support from the NSF (CHE-1955876) and computational resources from ACCESS through allocation TG-CHE180056. The TOC graphic, Figures 1 and 3, and Scheme 3 were created with Biorender.com. The authors wish to thank Dr. Eleanor Kearns and Prof. Deanna D'Alessandro, The University of Sydney, for assistance with cyclic voltammetry and useful discussions, Ms. Chianna Dane and Dr. Nicholas Proschogo, The University of Sydney, for assistance with high-resolution mass spectrometry, Dr. Lorna Wilkinson-White, Sydney Analytical, for assistance with SPR, Dr. Denise Tran and Dr. Ben Crossett, Sydney Mass Spectrometry, for assistance with LC–MS/MS, Dr. Yingying Su, Sydney Microscopy, for assistance with cellular imaging, Dr. Liam Adair, The University of Sydney, for advice regarding microscopy, and Ms. Zarwa Yaseen and Dr. Thomas Ashhurst, Sydney Cytometry, for assistance with mass cytometry. This research was facilitated by access to Sydney Analytical, Sydney Mass Spectrometry, Sydney Microscopy, and Sydney Cytometry, core research facilities at The University of Sydney. Open Access publishing facilitated by The University of Sydney, as part of the Wiley - The University of Sydney agreement via the Council of Australian University Librarians.

Conflict of Interest

The authors declare no conflict of interest.

Data Availability Statement

The data that support the findings of this study are available in the supplementary material of this article.

Keywords: Electrochemistry · Peptides · Proteins · Selenocysteine · Selenoethers

[1] a) A. C. Conibear, *Nat. Rev. Chem.* **2020**, *4*, 674–695; b) C. T. Walsh, S. Garneau-Tsodikova, G. J. Gatto Jr, *Angew. Chem. Int. Ed.* **2005**, *44*, 7342–7372.

[2] a) E. M. Sletten, C. R. Bertozzi, *Angew. Chem. Int. Ed.* **2009**, *48*, 6974–6998; b) O. Boutureira, G. J. L. Bernardes, *Chem. Rev.* **2015**, *115*, 2174–2195; c) J. N. deGruyter, L. R. Malins, P. S. Baran, *Biochemistry* **2017**, *56*, 3863–3873; d) C. D. Spicer, B. G. Davis, *Nat. Commun.* **2014**, *5*, 4740.

[3] a) E. A. Hoyt, P. M. S. D. Cal, B. L. Oliveira, G. J. L. Bernardes, *Nat. Rev. Chem.* **2019**, *3*, 147–171; b) O. Koniev, A. Wagner, *Chem. Soc. Rev.* **2015**, *44*, 5495–5551.

[4] a) V. V. Rostovtsev, L. G. Green, V. V. Fokin, K. B. Sharpless, *Angew. Chem. Int. Ed.* **2002**, *41*, 2596–2599; b) C. W. Tornøe, C. Christensen, M. Meldal, *J. Org. Chem.* **2002**, *67*, 3057–3064.

[5] N. J. Agard, J. A. Prescher, C. R. Bertozzi, *J. Am. Chem. Soc.* **2004**, *126*, 15046–15047.

[6] M. L. Blackman, M. Royzen, J. M. Fox, *J. Am. Chem. Soc.* **2008**, *130*, 13518–13519.

[7] a) L. J. Dowman, S. S. Kulkarni, J. V. Alegre-Requena, A. M. Giltrap, A. R. Norman, A. Sharma, L. C. Gallegos, A. S. Mackay, A. P. Welegedara, E. E. Watson, D. van Raad, G. Niederacher, S. Huhmann, N. Proschogo, K. Patel, M. Larance, C. F. W. Becker, J. P. Mackay, G. Lakhwani, T. Huber, R. S. Paton, R. J. Payne, *Nat. Commun.* **2022**, *13*, 6885; b) D. T. Cohen, C. Zhang, B. L. Pentelute, S. L. Buchwald, *J. Am. Chem. Soc.* **2015**, *137*, 9784–9787; c) D. T. Cohen, C. Zhang, C. M. Fadzen, A. J. Mijalis, L. Hie, K. D. Johnson, Z. Shriver, O. Plante, S. J. Miller, S. L. Buchwald, B. L. Pentelute, *Nat. Chem.* **2019**, *11*, 78–85; d) Z. Zhao, D. Shimon, N. Metanis, *J. Am. Chem. Soc.* **2021**, *143*, 12817–12824; e) L. Pedzisa, X. Li, C. Rader, W. R. Roush, *Org. Biomol. Chem.* **2016**, *14*, 5141–5147; f) J. Liu, Q. Chen, S. Rozovsky, *J. Am. Chem. Soc.* **2017**, *139*, 3430–3437; g) X. Li, C. G. Nelson, R. R. Nair, L. Hazlehurst, T. Moroni, P. Martinez-Acedo, A. R. Nanna, D. Hymel, T. R. Burke, C. Rader, *Cell Chem. Biol.* **2017**, *24*, 433–442, e436.

[8] a) Y. Weng, C. Song, C.-W. Chiang, A. Lei, *Commun. Chem.* **2020**, *3*, 171; b) M. Yan, Y. Kawamata, P. S. Baran, *Chem. Rev.* **2017**, *117*, 13230–13319; c) C. Zhu, N. W. J. Ang, T. H. Meyer, Y. Qiu, L. Ackermann, *ACS Cent. Sci.* **2021**, *7*, 415–431; d) D. Pollok, S. R. Waldvogel, *Chem. Sci.* **2020**, *11*, 12386–12400; e) A. S. Mackay, R. J. Payne, L. R. Malins, *J. Am. Chem. Soc.* **2022**, *144*, 23–41.

[9] a) Y. Lin, L. R. Malins, *Chem. Sci.* **2020**, *11*, 10752–10758; b) Y. Lin, L. R. Malins, *J. Am. Chem. Soc.* **2021**, *143*, 11811–11819; c) D. Alvarez-Dorta, C. Thobie-Gautier, M. Croyal, M. Bouzelha, M. Mével, D. Deniaud, M. Boujtita, S. G. Gouin, *J. Am. Chem. Soc.* **2018**, *140*, 17120–17126; d) S. Kitada, M. Takahashi, Y. Yamaguchi, Y. Okada, K. Chiba, *Org. Lett.* **2012**, *14*, 5960–5963; e) C. M. G. Lamb, J. Shi, J. D. Wilden, D. Macmillan, *Org. Biomol. Chem.* **2022**, *20*, 7343–7350; f) Y. Weng, X. Xu, H. Chen, Y. Zhang, X. Zhuo, *Angew. Chem. Int. Ed.* **2022**, *61*, e202206308; g) S. Sato, M. Matsumura, T. Kadonosono, S. Abe, T. Ueno, H. Ueda, H. Nakamura, *Bioconjugate Chem.* **2020**, *31*, 1417–1424; h) C. Song, K. Liu, Z. Wang, B. Ding, S. Wang, Y. Weng, C.-W. Chiang, A. Lei, *Chem. Sci.* **2019**, *10*, 7982–7987; i) S. Depienne, D. Alvarez-Dorta, M. Croyal, R. C. T. Temgoua, C. Charlier, D. Deniaud, M. Mével, M. Boujtita, S. G. Gouin, *Chem. Sci.* **2021**, *12*, 15374–15381; j) H.-C. Chen, C. Wan, W.-H. Shih, C.-Y. Kao, H. Jiang, Y. Weng, C.-W. Chiang, *Asian J. Org. Chem.* **2023**, *12*, e202200647.

[10] S. Nagahara, Y. Okada, Y. Kitano, K. Chiba, *Chem. Sci.* **2021**, *12*, 12911–12917.

[11] N. Metanis, E. Keinan, P. E. Dawson, *Angew. Chem. Int. Ed.* **2010**, *49*, 7049–7053.

[12] D. Giustarini, I. Dalle-Donne, A. Milzani, P. Fanti, R. Rossi, *Nat. Protoc.* **2013**, *8*, 1660–1669.

[13] a) World Health Organization Model List of Essential Medicines—22nd List. Geneva, **2021**; b) A. C. Wilson, S. Vadakkadath Meethal, R. L. Bowen, C. S. Atwood, *Expert Opin. Invest. Drugs* **2007**, *16*, 1851–1863; c) G. L. Plosker, R. N. Brogden, *Drugs* **1994**, *48*, 930–967.

[14] A. Orlova, M. Magnusson, T. L. J. Eriksson, M. Nilsson, B. Larsson, I. Höidén-Guthenberg, C. Widström, J. r Carlsson, V. Tolmachev, S. Ståhl, F. Y. Nilsson, *Cancer Res.* **2006**, *66*, 4339–4348.

[15] a) D. J. Slamon, G. M. Clark, S. G. Wong, W. J. Levin, A. Ullrich, W. L. McGuire, *Science* **1987**, *235*, 177–182; b) D. J. Slamon, W. Godolphin, L. A. Jones, J. A. Holt, S. G. Wong, D. E. Keith, W. J. Levin, S. G. Stuart, J. Udove, A. Ullrich, M. Press, *Science* **1989**, *244*, 707–712; c) N. Iqbal, N. Iqbal, *Mol. Biol. Int.* **2014**, *2014*, 852748; d) J. A. Freudenberg, Q. Wang, M. Katsumata, J. Drebin, I. Nagatomo, M. I. Greene, *Exp. Mol. Pathol.* **2009**, *87*, 1–11.

[16] a) J. H. Law, G. Habibi, K. Hu, H. Masoudi, M. Y. C. Wang, A. L. Stratford, E. Park, J. M. W. Gee, P. Finlay, H. E. Jones, R. I. Nicholson, J. Carboni, M. Gottardis, M. Pollak, S. E. Dunn, *Cancer Res.* **2008**, *68*, 10238–10246; b) S. E. O. Hye-Sook, K. U. Jin Mo, C. Han-Seok, W. O. O. Jong-Kyu, J. Bo-Hyoung, S. Yong Cheol, K. O. Seong-Gyu, *Anticancer Res.* **2014**, *34*, 2869–2882.

[17] a) C. H. Chau, P. S. Steeg, W. D. Figg, *Lancet* **2019**, *394*, 793–804; b) A. Beck, L. Goetsch, C. Dumontet, N. Corvaïa, *Nat. Rev. Drug Discovery* **2017**, *16*, 315–337; c) A. Thomas, B. A. Teicher, R. Hassan, *Lancet Oncol.* **2016**, *17*, e254-e262.

[18] S. Ståhl, T. Gräslund, A. Eriksson Karlström, F. Y. Frejd, P. -Å Nygren, J. Löfblom, *Trends Biotechnol.* **2017**, *35*, 691–712.

[19] a) L. Kambanis, T. S. Chisholm, S. S. Kulkarni, R. J. Payne, *Chem. Sci.* **2021**, *12*, 10014–10021; b) T. Koide, H. Itoh, A. Otaka, H. Yasui, M. Kuroda, N. Esaki, K. Soda, N. Fujii, *Chem. Pharm. Bull.* **1993**, *41*, 502–506; c) P. A. W. Dean, *Can. J. Chem.* **1979**, *57*, 754–761; d) V. Michelet, M. Savignac, J.-P. Genêt, in *Encyclopedia of Reagents for Organic Synthesis (EROS)*, Wiley, Hoboken, **2004**; e) J. P. Perdew in *Electronic Structure of Solids '91*. (Akademie Verlag, Berlin, **1991**); f) J. P. Perdew, J. A. Chevary, S. H. Vosko, K. A. Jackson, M. R. Pederson, D. J. Singh, C. Fiolhais, *Phys. Rev. B* **1992**, *46*, 6671–6687; g) A. D. Becke, *J. Chem. Phys.* **1993**, *98*, 5648–5652; h) V. A. Rassolov, M. A. Ratner, J. A. Pople, P. C. Redfern, L. A. Curtiss, *J. Comput. Chem.* **2001**, *22*, 976–984; i) M. M. Francl, W. J. Pietro, W. J. Hehre, J. S. Binkley, M. S. Gordon, D. J. DeFrees, J. A. Pople, *J. Chem. Phys.* **1982**, *77*, 3654–3665; j) P. C. Hariharan, J. A. Pople, *Theor. Chim. Acta* **1973**, *28*, 213–222; k) W. J. Hehre, R. Ditchfield, J. A. Pople, *J. Chem. Phys.* **1973**, *56*, 2257–2261; l) T. Clark, J. Chandrasekhar, G. W. Spitznagel, P. V. R. Schleyer, *J. Comput. Chem.* **1983**, *4*, 294–301; m) S. Grimme, J. Antony, S. Ehrlich, H. Krieg, *J. Chem. Phys.* **2010**, *132*, 154104; n) S. Grimme, S. Ehrlich, L. Goerigk, *J. Comput. Chem.* **2011**, *32*, 1456–1465; o) J. K. Pearson, F. Ban, R. J. Boyd, *J. Phys. Chem. A* **2005**, *109*, 10373–10379; p) G. S. Heverly-Coulson, R. J. Boyd, *J. Phys. Chem. A* **2011**, *115*, 4827–4831; q) E. Cancès, B. Mennucci, J. Tomasi, *J. Chem. Phys.* **1997**, *107*, 3032–3041; r) B. Mennucci, E. Cancès, J. Tomasi, *J. Phys. Chem. B* **1997**, *101*, 10506–10517; s) G. Scalmani, M. J. Frisch, *J. Chem. Phys.* **2010**, *132*, 114110; t) J. Tomasi, B. Mennucci, E. Cancès, *J. Mol. Struct.* **1999**, *464*, 211–226; u) B. Mennucci, J. Tomasi, *J. Chem. Phys.* **1997**, *106*, 5151–5158; v) A. V. Marenich, C. J. Cramer, D. G. Truhlar, *J. Phys. Chem. B* **2009**, *113*, 6378–6396; w) J. V. Alegre-Requena, S. Sowndarya, R. Pérez-Soto, T. M. Alturaifi, R. S. Paton, *WIREs Comput. Mol. Sci.* **2023**, *13*, e1663; x) M. J. Frisch, G. W. Trucks, H. B. Schlegel, G. E. Scuseria, M. A. Robb, J. R.

Cheeseman, G. Scalmani, V. Barone, G. A. Petersson, H. Nakatsuji, X. Li, M. Caricato, A. V. Marenich, J. Bloino, B. G. Janesko, R. Gomperts, B. Mennucci, H. P. Hratchian, J. V. Ortiz, A. F. Izmaylov, J. L. Sonnenberg, Williams, F. Ding, F. Lipparini, F. Egidi, J. Goings, B. Peng, A. Petrone, T. Henderson, D. Ranasinghe, V. G. Zakrzewski, J. Gao, N. Rega, G. Zheng, W. Liang, M. Hada, M. Ehara, K. Toyota, R. Fukuda, J. Hasegawa, M. Ishida, T. Nakajima, Y. Honda, O. Kitao, H. Nakai, T. Vreven, K. Throssell, J. A. Montgomery Jr, J. E. Peralta, F. Ogliaro, M. J. Bearpark, J. J. Heyd, E. N. Brothers, K. N. Kudin, V. N. Staroverov, T. A. Keith, R. Kobayashi, J. Normand, K. Raghavachari, A. P. Rendell, J. C. Burant, S. S. Iyengar, J. Tomasi, M. Cossi, J. M. Millam, M. Klene, C. Adamo, R. Cammi, J. W. Ochterski, R. L. Martin, K. Morokuma, O. Farkas, J. B. Foresman, D. J. Fox, *Gaussian 16 Rev. C.01*, Wallingford, CT, **2016**; y) K. Fukui, *Acc. Chem. Res.* **1981**, *14*, 363–368; z) S. Grimme, *Chem. Eur. J.* **2012**, *18*, 9955–9964; aa) G. Luchini, J. Alegre-Requena, I. Funes-Ardoiz, R. Paton, *F1000Research* **2020**, *9*, 291; ab) V. S. Bryantsev, M. S. Diallo, W. A. Goddard III, *J. Phys. Chem. B* **2008**, *112*, 9709–9719; ac) H. G. Roth, N. A. Romero, D. A. Nicewicz, *Synlett* **2016**, *27*, 714–723.

Manuscript received: September 4, 2023
Accepted manuscript online: October 11, 2023
Version of record online: November 9, 2023